ABLATING AND CHARRING OF TWO DIMENSIONAL HEAT SHIELD MATERIALS

Mohammad Reza Shabani[1] and Mohammad Hassan Rahimian[2*]

The objective of this research is to estimate two dimensional ablating and charring of heat shield materials in severe aero-thermal heat transfer. This estimation requires an accurate and rapid technique for its serious heat transfer with a moving boundary. Aerodynamic heating is obtained by an explicit relation which is a function of Mach number and air condition, while a fully implicit method is used for heat transfer calculations. Moving boundary is captured by FLIAR method which is a subgroup of VOF. Thickness of ablating and charring of heat shield, temperature of the moving surface and rate of radiation heat are calculated and compared with references. The results are in good agreement with other calculations.

Keywords: Ablating, Charring, Heat Shield, Pyrolysis, Aero Thermal, VOF Method

1. INTRODUCTION

Ablating and charring of heat shield materials in severe rate of heat transfer is needed in the designing of reentry vehicles, metal casting and nuclear reactor operations. Applying a finite difference technique, Landau et al.[1] solved the ablation speed in a semi-infinite solid subject to a uniform heat flux or convection at the boundary. Recession of the domain was applied by regrid method. Regrinding of the domain is easy in one dimensional media while, in two dimensional domain regrinding is an important problem. Goodman[2] and Altman[3] used the heat balance integral method (HBI) in a one dimensional domain. Zien[4] proposed the θ -momentum integral method to treat one- dimensional transient ablation. Potts[5] used the quasi-steady and heat balance integral method to consider this phenomenon. Quasi-steady state model is poor for this object and finite difference method with regriding in spite of good accuracy, is too slow to use in large parametric studies. In this work finite difference method is used to solve two dimensional governing equations and the FLAIR method[6] is applied to capture the recession of the surface instead of regriding of the domain. This method reduce the necessary nodes about 75% and run time of the code reduced about 70% for one dimensional media so for 2-D consuming time will be decreased seriously. In the FLAIR method a matrix F is defined in the whole solution domain. F is equal to one in non-ablated cells and equal to zero in ablated cells. F is between one and zero in the surface cells. In this paper phenomenological study of charring and ablating of heat shield materials is considered, too. The charring ablator material is a composite of carbon-phenolic.

Received: August 4, 2004, Accepted: January 24, 2005.

1 Graduate Student, Mechanical Eng. Department, Faculty of Eng., University of Tehran, Tehran, Iran.

2 Assistant Professor, Mechanical Eng. Department, Faculty of Eng., University of Tehran, Tehran, Iran.

* Corresponding author. E-mail: rahimyan@ut.ac.ir

2. ANALYSIS OF CARBON-PHENOLIC CHARRING ABLATOR MODEL

Carbon-phenolic heat shields consist of layers of carbon fabric saturated with a phenolic resin. When Carbon-phenolic is heated, and the temperature sufficiently elevated, the resin begins to decompose, yielding a pyrolysis gas containing water, carbon oxides, lower hydrocarbons, and a carbon residue. This carbon residue and the carbon cloth around it, is called "char" undecomposed material is termed "virgin".

The resin breakdown into pyrolysis gases consists of a series of primarily endothermic chemical reactions, which soak up large amounts of

energy. A reaction zone is set-up below the surface of the material, which can experience significant density gradients and changes in temperature of several hundred degrees per second. The gaseous pyrolysis products from the in-depth reaction zone transpire or get into the nearer-surface porous charred material, absorbing additional energy.

While the reaction zone moves deeper into the body, the charred outer surface becomes sufficiently hot to re-radiate energy back into the boundary layer. The venting of the pyrolysis gases into the boundary layer also blocks some of the incident heat (this is called boundary layer "blowing"). The charred outer surface also usually becomes hot enough to ablate by means of carbon oxidation and sublimation. Here, the injection of pyrolysis gases greatly affects the carbon oxidation and sublimation rates.[7,8]

3. Governing Equations and Boundary Conditions

Although for many applications of heat shield configurations, a one-dimensional model suffices, but to obtain a good accuracy a two dimensional model is needed. The standard in-depth governing equations for two-dimensional charring ablator response are as follows.

Decomposition:

$$\frac{\partial \rho}{\partial t} = -\rho_v \left(\frac{\rho - \rho_c}{\rho_v - \rho_c}\right)^n \sum_j A_j \exp(-B_j / T) \tag{1}$$

Continuity (Mass):

$$\frac{\partial \dot{m}_{gx}}{\partial x} + \frac{\partial \dot{m}_{gy}}{\partial y} = \frac{\partial \rho}{\partial t} \tag{2}$$

Energy:

$$\frac{\partial(\rho h)}{\partial t}\Big|_{x,y} = \frac{\partial}{\partial x}\left(k_{XX}\frac{\partial T}{\partial x} + k_{XY}\frac{\partial T}{\partial y}\right) + \frac{\partial}{\partial y}\left(k_{YX}\frac{\partial T}{\partial x} + k_{YY}\frac{\partial T}{\partial y}\right) + \frac{\partial}{\partial x}\left(\dot{m}_{g_X}\left(h_P + h_g\right)\right) + \frac{\partial}{\partial y}\left(\dot{m}_{gy}\left(h_P + h_g\right)\right) \tag{3}$$

For isotropic media when properties change with temperature, the energy equation becomes:

$$\frac{\partial(\rho C_P T)}{\partial t}\Big|_{x,y} = K\frac{\partial^2 T}{\partial x^2} + K\frac{\partial^2 T}{\partial y^2} + \frac{\partial K}{\partial x}\frac{\partial T}{\partial x} + \frac{\partial K}{\partial y}\frac{\partial T}{\partial y} + C_{pg}\left[\dot{m}_{gX}\frac{\partial T}{\partial x} + \dot{m}_{gy}\frac{\partial T}{\partial y}\right] + \Delta h_{pg}\frac{\partial \rho}{\partial t} \tag{4}$$

where, $\Delta h_{pg}$is heat of pyrolysis per unit mass of gas produced, j/g, $\dot{m}_g$ is mass flux of pyrolysis gas, g/(cm^{2}s), $C_{pg}$is specific heat of pyrolysis gas, j/(g k). The heat of pyrolysis per unit mass of gas produced at the local temperature is[9]

$$\Delta h p_g = h_g - (\rho_v h_v - \rho_c h_c)/(\rho_v - \rho_c) \tag{5}$$

Here, enthalpies for virgin, char, and gaseous matter are:

$$h_i = \Delta h_{f,i} + \int_{Tref}^{T} cp_i dT \tag{6}$$

In general, the heat shield surface goes back due to ablation. Ablation refers to the sacrificial mass loss of heat-laden outer surface material via thermochemical reaction, thereby keeping the interior relatively cool. The velocity of recession is consisting of erosion and ablating surface. In this paper erosion is neglected so:

$$\dot{S} = \dot{S}_{ab}\,,\ \dot{S}_{ab} = \dot{m}_{ab}/\rho_w \tag{7}$$

A surface energy balance yields the net heat flux conducted into the surface. Application of Fourier's Law produces the front-face boundary condition at the moving surface.

$$-K\vec{\nabla}T.\vec{n} = \dot{q}_{net} \tag{8}$$

Mechanisms are oxidation and sublimation of solid carbon, with no melting or liquid layer formation; there is only a gaseous phase adjacent to a solid, reacting surface. Conservation of mass requires (Fig. 1-d)

$$\dot{q}_{net} = \dot{q}_{conv} - \dot{q}_r - \dot{m}_{ab}(h_w - h_u) - \dot{m}_{gw}(h_w - h_{gw}) \tag{9}$$

$$\dot{m}_w = \dot{m}_u + \dot{m}_{gw} \tag{10}$$

where the first term $\dot{m}_w$ is the mass transfer rate

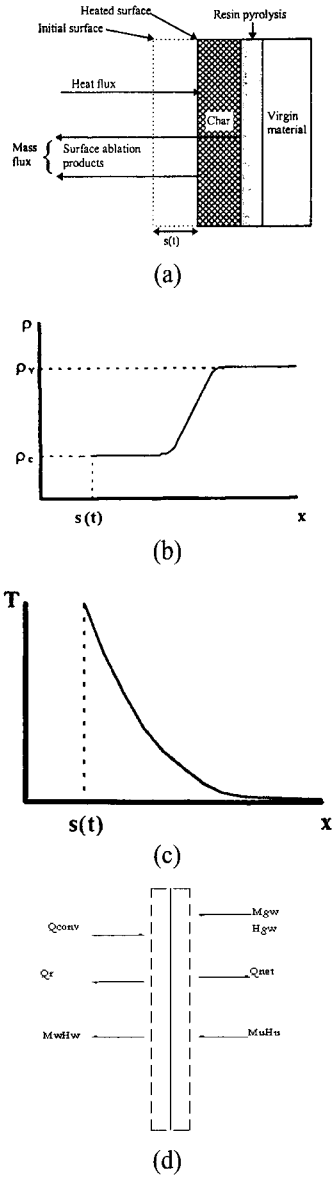

Fig. 1 Heat and mass transfer with pyrolysis, typical density temperature distributions and surface energy balance

into the boundary layer, the mass flux of solid material disappearing from the heat shield surface is assumed to consist of a thermochemical ablation

$$\dot{m}_u = \dot{m}_{ab} \tag{11}$$

Substitution of Eq. (10) into Eq. (9) produces

$$\dot{m}_w = \dot{m}_{ab} + \dot{m}_{gw} \tag{12}$$

Conservation of energy requires:

$$\dot{q}_{net} = \dot{q}_{conv} - \dot{q}_r - \dot{m}_{ab}(h_w - h_u) + \dot{m}_{gw}(h_w - h_{gw}) \tag{13}$$

The convective heat flux includes both the conductive and inter-diffusional energy fluxes across the left and right of control surface, and is correlated as.[7]

$$\dot{q}_{conv} = g_h(h_r - h_w) \tag{14}$$

g_h is a heat transfer coefficient and h_r is recovery enthalpy. Standard aeroheating correlation[6] provides recovery enthalpy h_r, boundary layer edge or wall pressure p_e, heat transfer coefficient to a non-ablation wall g_{h0}, and enthalpy of air at the wall temperature h_{w0}. Because of the injection of ablation products into the boundary layer, g_h must be modified by a blowing correction to produce g_h. Also the reaction of ablation products with boundary layer gases, h_{w0} must be modified to produce h_w.[7]

$$g_h = g_{h_o} \cdot \Phi_{blow}$$

The heat flux re-radiated away from the surface is presumed to be:

$$\dot{q}_r = \varepsilon\sigma(T_w^{\ 4} - T_{ref}^{\ 4}) \tag{15}$$

Carbon-phenolic surface emissivity ranges between 0.6 and 0.85 for application of interest. In this paper $\varepsilon = 0.85$.

4. SURFACE TRACKING METHOD

A conventional volume tracking method using a marker function, along with an efficient interface curvature determination technique called, the Flux Line Segment Model for Advection and Interface Reconstruction (FLAIR) proposed by Ashgriz and Poo,[6] are used to capture the moving surface. To track this moving surface a void fraction marker function is defined over the entire field. The method requires an evenly spaced grid intervals resulting in a square cell two-dimensional mesh. The value of the void fraction function ranges from zero for empty cells to one for filled cells. The

ablating geometry provides the means by which the value of the void fraction function is determined in each cell. The surface line in a boundary cell determines the fraction of the space occupied by the ablating material. This is the value of the void fraction function in that cell. The advection of this surface line segment through the field determines the recession of heat shield. All possible surface line position between two adjacent cells are considered and an algorithm for relating advection of surface from one cell to it's neighboring cell is obtained through the solution of the transport of the void fraction function in the flow field, governed by the equation $\partial F/\partial t + \vec{V} \bullet \nabla F = 0$. Ashgriz and Poo[6] provide a complete description of the theory and application of this method.

5. Solution Method

In order to solve the governing equations a uniform and fixed grid is used inside the domain. Moving of the outer surface versus time imposes a time dependent boundary condition. Therefore, the distance of surface cell is changed and finite difference relation in non-uniforcm grid is used as bellow:

$$\left(\frac{\partial T}{\partial X}\right)_{i,j} = \left[-T_{i-1,j} + (1-(\overline{F_x})^2)T_{i,j} + (\overline{F_x})^2 T_{i+1,j}\right] B_x, \left(\frac{\partial^2 T}{\partial X^2}\right)_{i,j}$$

$$= \left[-T_{i-1,j} + (1-\overline{F_x})T_{i,j} + \overline{F_x} T_{i+1,j}\right](2B_x / H)$$

where

$$\Delta X^+ = \left(\frac{f_{i,j} + f_{i+1,j}}{2}\right)H, \quad \Delta X^- = \left(\frac{f_{i-1,j} + f_{i,j}}{2}\right)H,$$

$$\overline{F_x} = \frac{\Delta X^+}{\Delta X^-}, \quad \overline{F_Y} = \frac{\Delta Y^+}{\Delta Y^-}$$

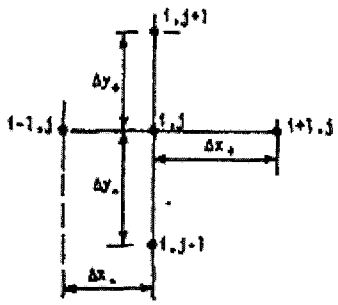

Fig. 2 Stencil of surface cell

$$\Delta Y^- = \left(\frac{f_{i,j} + f_{i,j-1}}{2}\right)H, \quad \Delta Y^+ = \left(\frac{f_{i,j} + f_{i,j+1}}{2}\right)H,$$

$$B_x = \frac{1}{(\overline{F_x}H)(1+\overline{F_x})}$$

His the fixed space between cells.

Equation of conservation of mass inside the domain is applied as:

$$\left(\frac{\partial \dot{m}_{gx}}{\partial X}\right)^{n+\frac{1}{2}} = \left(\frac{\partial \rho}{\partial t}\right)^{n+\frac{1}{2}} - \left(\frac{\partial \dot{m}_{gy}}{\partial Y}\right)^{n}$$

$$\left(\frac{\partial \dot{m}_{gy}}{\partial Y}\right)^{n+1} = \left(\frac{\partial \rho}{\partial t}\right)^{n+1} - \left(\frac{\partial \dot{m}_{gx}}{\partial X}\right)^{n+\frac{1}{2}}$$

Discretization of Arrhenius model in two dimensional domain is as:

$$\left(\frac{\partial \rho}{\partial t}\right)^{n+\frac{1}{2}} = -\rho_v \left(\frac{\rho^{n+\frac{1}{2}} - \rho_c}{\rho_v - \rho_c}\right)^n \sum_j A_j \exp(-B_j / T_{i,j}^{n+\frac{1}{2}})$$

$$\left(\frac{\partial \rho}{\partial t}\right)^{n+1} = -\rho_v \left(\frac{\rho^{n+1} - \rho_c}{\rho_v - \rho_c}\right)^n \sum_j A_j \exp(-B_j / T_{i,j}^{n+1})$$

Using Crank-Nicolson method to solve energy equation as :

$$A'_i T_{i-1,j}^{n+\frac{1}{2}} + B'_i T_{i,j}^{n+\frac{1}{2}} + C'_i T_{i+1,j}^{n+\frac{1}{2}} = D'_i$$

$$A''_j T_{i,j-1}^{n+1} + B''_j T_{i,j}^{n+1} + C''_j T_{i,j+1}^{n+1} = D''_j$$

The system of equation solved by A.D.I. method.

6. Results and Discussion

To show the general robustness of one dimensional code, VOF, a regrid finite difference method is used and compared with references. The interested reader referred to Rahimian and Shabani.[8] The schematic of heat shield is shown in fig 1. It consists of virgin, pyrolysis, charring heat surface zone and the ablated area, which is eliminated from the computational domain.

Fig. 3 shows a two dimensional heat shield which is subject to aero-thermal heat transfer. The domain is a semi-cylinder and it is divided into

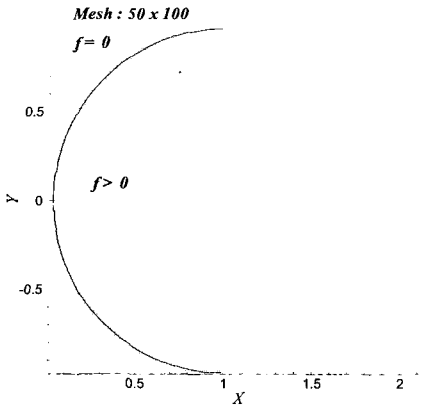

Fig. 3 Computational Domain for Heat Transfer

200*400 cells. This section is divided into two parts, first part discuses to approve two dimensional code and second part applies a real 2-D heat flux to a semi-cylinder nose.

6.1 VERRIFICATION OF 2-D CODE

Because there is no experimental or numerical results for two dimensional domain the code will be verified by the following ways

1- Grid independency of the code
2- Comparison of the reslts with one dimensional results
3- Using a uniform heat flux to a 2-D domain and obtaining parallel surface recession and parallel temperature contours.

Fig. 5 shows grid independency of the two dimensional code. It is run for 100x200, 200x400 and 300x600 grids. Surface temperature of 2-D heat shield is compared with one dimensional results. As seen grid independency is achieved for 200x400 grids.

To approve 2-D code it is wise to compare the results with one dimensional domail, if the uniform-heat flux imposed to the surface. On the hand while temperature contours and recession of the surface in the semi-cylinder is parallel the results are acceptable. Fig. 4 shows the parallel temperature contours at the 27 th and 34 th secomds.

Although 2-D results are in good agreement with results of 1-D, Temperature in 2-D is about 2% over than 1-D. It is obvious that the ratio of surface to volume for a convex shape is more than in a flat wall. Therefore total heat transfer per volume in a convex shape will be more than in a flat wall and temperature increase about 2%.

Fig. 6 indicates the convection heat flux on the external surface, with cold wall temperature boundary condition and ablating surface. Heat flux has grown slowly in the 21st seconds and increased from 21st second up to its maximum and then decrease until the end of the program time. This is an input of the code, which is used for stagnation point and obtained from standard aerodynamics relations for one-dimensional domain and is applied to 2-D media. The second boundary condition, ablating surface, occurs when temperature is going up and blowing gases prevent heat transfer. In this boundary condition convection heat flux decreased

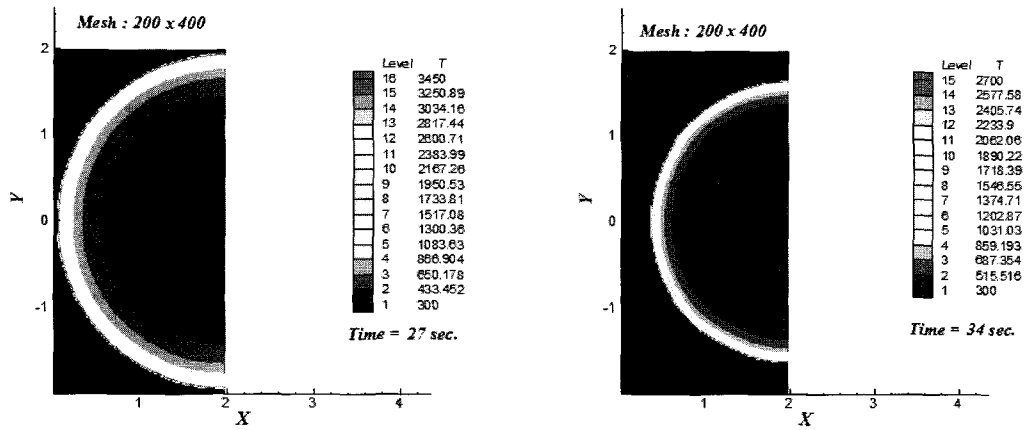

Fig. 4 Temperature Contour for 2-D at time t=27 and 34

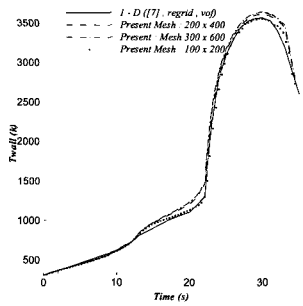

Fig. 5 Temperature distribution versus time

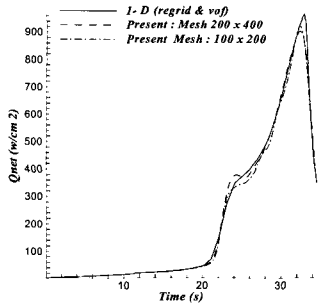

Fig. 8 Net heat flux versus time

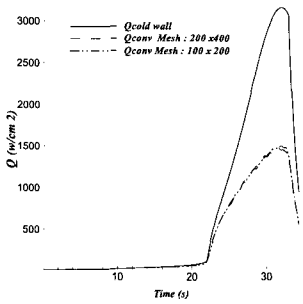

Fig. 6 Convection heat flux

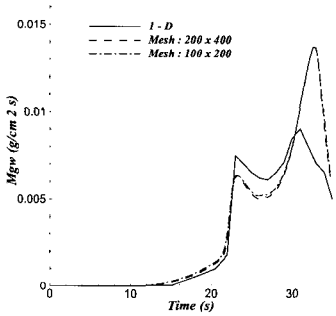

Fig. 9 Mass flux of pyrolysis gas

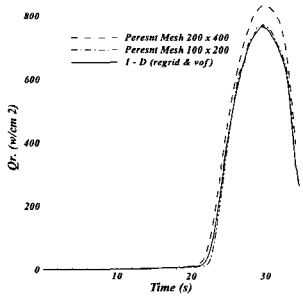

Fig. 7 Radiated heat flux versus time

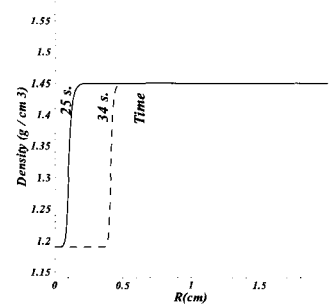

Fig. 10 Gradient of density in domain

more than 50% from its maximum.

The heat flux re-radiated away from the surface and net heat flux conducted into the heat shield is shown in Fig. 7 and 8 respectively. Increasing wall temperature in two-dimensional domain causes increasing in re-radiated heat and therefore net heat flux decreases. Fig. 9 denotes mass pyrolysis gas flux from the surface versus time in one and two-dimensional domain. Penetration of temperature in two-dimensional domain is more than its value in 1-D, so mass of gas flux arise after 30 second comparing with one dimensional domain. High gradient of temperature and density is observed in Fig. 10. As seen, high gradient of density is occurred in pyrolysis zone severely in all times. Fig. 11 demonstrates regression of the surface for one and two-dimensional domain. As expected due to high temperature of two-dimensional domain its recession increased about 5%. Recession of the surface in the semi-cylinder which is parallel at three times is shown in Fig. 12.

6.2 Application of 2-D Geometry

Aerodynamic heating will be changed with angle of the surface. It means that maximum heating occurs in the stagnation point, when angle of the surface is equal to zero degrees and heating is

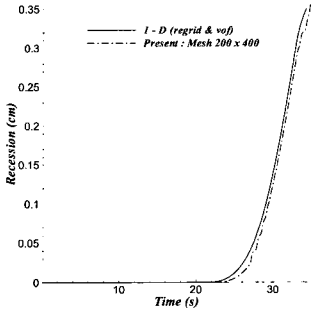

Fig. 11 Recession of the heated surface

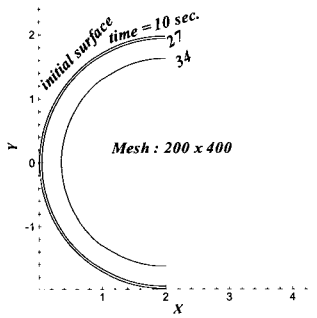

Fig. 12 Profile of surface at different time

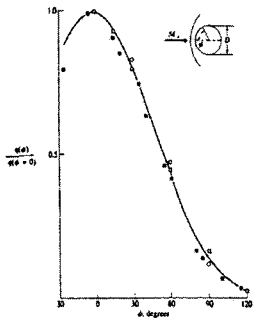

Fig. 13 Variation of heat flux versus angle of the surface

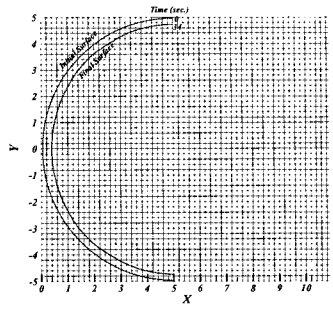

Fig. 14 Comparison of the surface of heat shield at time t=0.0 and t=34s

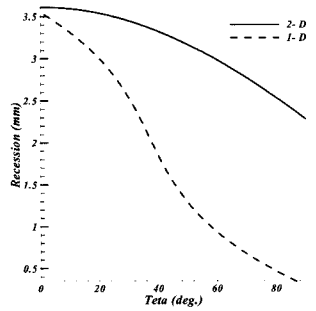

Fig. 15 Recession versus angle of the surface for 1D and 2D

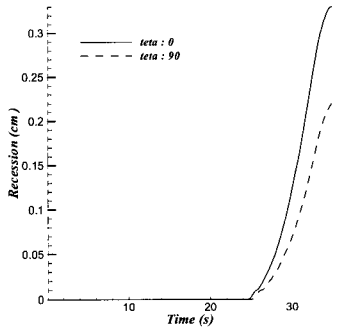

Fig. 16 Recession for two angles versus time

minimum when angle of the surface is equal to 90 degrees. The dissimilarity of heat flux imposed to the semi cylinder is shown in Fig. 13. In this section by imposing this heat flux, the bellow results are obtained.

Fig. 14 shows the comparison of the surface at two times, t = 0.0 and t = 34 s. Maximum recession is about 3.59 mm occurred in the stagnation point where angle of the surface is equal to zero and minimum recession is about 2.25 mm at $\theta = 90$ degrees. Minimum to maximum recession ratio is equal to 0.62 while the ratio of heat flux is about 0.15. If this heat flux imposed to 1-D code maximum recession will be about 3.55 mm and the minimum will reach to about .27 mm. In 1-D code minimum to maximum recession ratio is equal to 0.08. (see Fig. 15). Fig. 16 shows minimum and maximum recession of the surface versus time. Although these recessions started at the same time, i.e. 21st second, minimum recession is about half of

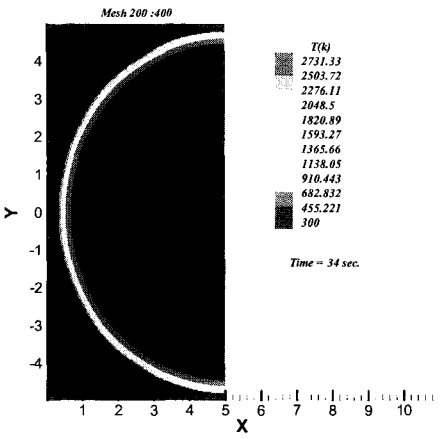

Fig. 17 Recession of the surface and temperature contours

the maximum at the end time. Recession and temperature contours for t=34 s are shown in Fig. 17.

REFERENCES

[1] Landa, H.G., 1950, "Heat Conduction in a melting solid," *Quarterly Applied Mathematics*, Vol.8, No.1, pp.312 -319.

[2] Goodman, T.R., 1958, "The Heat Balance integral and its application to problems involving a change of phase," *Transactions of the ASME*, Vol.80, pp.315-322.

[3] Altman, M., 1961, "Some Aspects of the Melting Solution for a Semi Infinite Slab," *Chemical Engineering Progress Symposium Series*, Vol.57, pp.16-23.

[4] Zien, T.F., 1978, "Integral Solution of Ablation Problems with Time Dependent Heat Flux," *AIAA, Journal*, Vol.16, pp.1287-1295.

[5] Potts, R.L., 1990, "Hybrid Integral/Quasi – Steady Solution of Charring Ablation," *AIAA Paper 80-1688.*

[6] Ashgriz, N. and Poo, 1991, "FLAIR – Flux Line Segment Model For Advective and Interface Reconstruction," *Journal of Comp. Phys.*, No.2, p.444.

[7] Potts, R.L., 1995, "Application of Integral Methods," *SPASECRAFT AND ROCKETS*, Vol.2, No.4.

[8] Rahimian, M.H. and Shabani, M.R., 2003, "Ablating and Charring of Heat Shield Materials," *Proceeding of CFD 2003 CANADA.*